MEDDOCS Open Access Publisher

Nanoscience and Nanotechnology: Open Access

Open Access | Research Article

Formulation and Evaluation of GMO Based Nanoparticulate Carriers for Percutaneous Delivery of Anti-Inflammatory Drug

Corresponding Author(s): M Kishore Babu

Professor and Principal, Krishna Teja Pharmacy College, Chadalawada Nagar, Renigunta Road, Tirupati- 517506.

Email: Kishorecollagen@gmail.com

Received: May 08, 2023

Accepted: May 30, 2023

Published Online: June 06, 2023

Journal: Nanoscience and Nanotechnology: Open Access

Publisher: MedDocs Publishers LLC

Online edition: http://meddocsonline.org/

Keywords: Lornoxicam; Nanoparticulate carriers; Anti-inflammatory.

Abstract

Context: The usage of Lornoxicam is mainly constrained by its shorter biological half-life and associated side effects like gastric irritation and peptic ulcer when given orally. The present research is primarily focused on formulation of GMO based liquid crystalline nanoparticles for percutaneous administration of lornoxicam for sustaining the drug release and amelioration of profound side effects leading to better therapy.

Objective: The main objective of this research activity is to formulate GMO based liquid crystalline nanoparticles for percutaneous administration of Lornoxicam for better management against musculo-skeletal and joint disorders like rheumatoid arthritis and osteoarthritis.

Methods: Lornoxicam liquid crystalline nanoparticles were formulated by employing emulsification followed by high-speed homogenization technique. Particle size, zeta potential and polydispersity index were determined using photon correlation spectroscopy whereas particle morphology and structural organization were determined using TEM. Percentage entrapment efficiency and cumulative % drug release were assessed.

Conclusion: Based on the results it could be concluded that formulation F_4 can be considered as the better formulation for the effective management of rheumatoid arthritis and osteoarthritis.

Introduction

Lornoxicam is a non-steroidal anti-inflammatory drug categorised under oxicam derivatives which is used in treatment of mild to moderate pain and inflammation for musculo-skeletal and joint disorders like rheumatoid arthritis, osteoarthritis and ankylosing spondylitis [1]. Inspite of its profound side effects like gastric irritation and peptic ulcer, Lornoxicam is preferred over other oxicam derivatives piroxicam, tenoxicam and other NSAIDS like tramadol as it has great analgesic potency [2,3]. Lornoxicam acts by inhibition of cyclooxygenase enzyme and interferes with the prostaglandin synthesis at peripheral cell damage sites and it also has a direct action on spinal nociceptive processing which boosts up the peripheral mechanism attributing to inhibition of COX activity [4,5]. Percutaneous delivery of Lornoxicam will avert the aforementioned side effects as well as provide better therapeutic efficacy. Although there are other approaches for sustaining the drug release like formulating as PLGA Microspheres [6], the aqueous solubility could be enhanced by formulating as GMO based liquid crystalline nanoparticles.Since their inception, LCNP's have been quite intriguing for many scientists due to their unique capability of incorporating amphiphilic, hydrophilic and hydrophobic drugs [7]. Luzzati and Hasson first identified the presence of liquid crys-

Cite this article: Kishore Babu M. Formulation and Evaluation of GMO based Nanoparticulate carriers for Percutaneous delivery of Anti-inflammatory drug. Nanosci Nanotechnol Open Access. 2023; 2(1): 1011.

talline phases in self-assembly lipid-water systems [8]. These liquid crystalline phases existed in sponge, bicontinuous cubic, reverse micellar cubic and reverse hexagonal phases. Among which the aqueous dispersions of bicontinuous cubic (cubosomes) [9] and reverse hexagonal phases(hexosomes) [10] gained attention as they exhibited a cavernous honey combed structure offering large interfacial area for accommodating variety of drugs [11]. Glyceryl monooleate has been selected as key excipient due to its biocompatible, biodegradable and non-toxic properties [12,13] .Moreover the GMO acts as penetration enhancer by promoting ceramide extraction and enhancement of lipid fluidity in the stratum corneum [14]. The penetration of the drugs through the skin and their percutaneous delivery are limited by the barrier function of the highly organized structure of stratum corneum [15]. Liquid crystalline nanoparticles in particular cubosomes and hexosomes have shown to improve the topical delivery of drugs. The more penetration of cubosomes is due to the structural similarity with that of stratum corneum [16] where as in case of hexosomes it may be attributed to the extraction of lipids present in the skin [17].

Materials & Methods

Materials

Lornoxicam was obtained as a gift sample from Glenmark Pharmaceuticals Ltd, Mumbai, India. Glyceryl Monooleate was procured from Sigma-Aldrich, Bangalore, India and Lutrol F-127 was procured from Himedia Laboratories, Mumbai.

Formulation of Glyceryl monooleate based liquid crystalline nanoparticles loaded with lornoxicam:

LCNP dispersions were produced by Emulsification of varying concentrations of Glyceryl monooleate and Lutrol F127 in water (95% w/w), followed by subsequent sonication and homogenization as described by Esposito.et al [8]. In the present study, 50 mg of drug was added to molten GMO (4-4.8% w/w) and Lutrol F127 (0.2-1% w/w) [19] **(Table 1)** solution and solubilized completely prior drop-wise addition into 47.5ml of water (95% w/w) under mechanical stirring using a stirrer (Remi instruments ltd, Mumbai, India) at 1500 rpm. Stirring was continued for 2 hours at room temperature. Later the dispersions were subjected to sonication using tip probe sonicator (Vibra cell) at (80% energy intensity, 30 seconds pulse on and 30 seconds pulse off) for 20 minutes with ice water bath maintained at 4°C for uniform mixing, followed by subsequent homogenization at 15000 rpm (Ika Ultra turrax T25, Mumbai) at 60oC for 5 minutes. After cooling, the dispersions were stored in glass vials covered with aluminium foils and maintained at room temperature.

Physical characterization of Dispersions

Photon correlation spectroscopy

The mean hydrodynamic diameter (Z-average,nm), Polydispersity index and zeta potential(mV) were investigated using Nanoparticle Analyzer (Nanopartica SZ-100, Horiba scientific, Japan). The dispersion samples were diluted appropriately with deionized water and measurements were carried out at 25°C at a laser wavelength of 659.0nm and a scattering angle of 173º with a run time of 60 seconds [20]. The samples were vortexed prior measuring the particle size, Polydipersity index (PDI) and zeta potential. The values obtained were represented in **Table 1**. The data was interpreted by method of cumulants. Based on National Institute standard, a sample with a PDI<0.05 was considered to be monodispersed [21]. Polydispersity index is given by the following equation:

$PdI = (\sigma/d)^2$

σ – Standard deviation

d – Mean diameter (Z-average)

Transmission Electron Microscopy

Samples were vortexed for half an hour prior placing a 5µl sample on 300 mesh carbon grids. The excess fluid was removed by wicking it off with an absorbent paper. The samples were negatively stained with 1% uranyl acetate. These grids were given enough time for drying up before viewing in Transmission electron microscope [22]. The electron photomicrographs of samples were taken using Tecnai 20T (FEI) TEM at 200kV. Photomicrographs were taken in both imaging and diffraction modes.

Determination of Drug Entrapment Efficiency

10 ml of dispersion was transferred into 15ml centrifuge tube and subjected to centrifugation at 16,000 rpm at 4°C using remi cooling centrifuge, Model-C23 (Remi instruments Ltd, Mumbai, India) for 1hr .The clear supernatant was diluted appropriately with 7.4 pH phosphate buffer and the amount of the drug unentrapped was estimated at 376nm using UV-Visible spectrophotometer (Shimadzu-1700).The Entrapment Efficiency **(Table 1)** was determined as follows [19]:

% Entrapment efficiency (%EE) = (Amount of entrapped drug/ Amount of feed drug) x 100.

Invitro diffusion studies: Invitro diffusion studies of prepared dispersions were performed using Modified Franz diffusion cell with a receiver compartment

Volume of 15ml and effective diffusion area of 2.50cm^2. A dialysis membrane having a pore size of 2.4nm with a molecular weight cut-off range of 12000-14000daltons was used in the present study. The membrane was soaked in double distilled water for 12 hours prior mounting horizontally between receptor and donor compartments. The receptor compartment was filled with 15ml of 7.4pH phosphate buffer and thermostated at 37±0.5 °C. This solution was stirred using a magnetic bar at 100rpm during entire experiment. A volume of LCNP'S dispersion of Lornoxicam was placed in the donor compartment. Aliquots (3ml) were withdrawn at regular intervals for 72 hours from receptor compartment and replaced by fresh medium to maintain sink conditions. The samples were diluted appropriately with buffer medium and analysed by U.V-Visible spectrophotometer (Shimadzu-1700, Mumbai) at 376nm [18,23].

Results

Different formulations of lornoxicam liquid crystalline nanoparticles were prepared by emulsification followed by homogenization technique by varying the concentrations of GMO and Lutrol F-127 and evaluated for Particle size distribution, Zeta potential, Entrapment efficiency, Cumulative drug release and particle morphology respectively. The composition data is represented in **Table 1**. The values obtained for Particle size distribution **(Figure 1(A)to 1(I))**, Zetapotential **(Figure 2(A) to 2(I)** and % Entrapment efficiency are represented in **Table 1** and the responses for % Cummulative drug release **(Figure 5)** and diffusion kinetics are represented in **Table 2 and Table 3** respectively. TEM micrographs are represented in Figure 3(A) to 3(H) respectively and selected area diffraction pattern of formula-

tion F9 is represented as **Figure 4**.

Table 1: Composition, Z-average, PDI, Zetapotential & % Entrapment efficiency of formulations (F_1-F_9).

Formulation code	Drug (mg)	GMO (% w/w)	Lutrol F127 (% w/w)	Water (% w/w)	Z-average (nm)	PDI	Zeta potential	%EE
F_1	50	4.8	0.2	95	367.9	0.0594	-23.3	60.92
F_2	50	4.7	0.3	95	366.2	0.0614	-26.1	58.28
F_3	50	4.6	0.4	95	304.3	0.083	-28	56.9
F_4	50	4.5	0.5	95	263.9	0.0758	-32.1	54.75
F_5	50	4.4	0.6	95	256.2	0.1054	-33.1	52.03
F_6	50	4.3	0..7	95	234.9	0.2635	-34.4	50.69
F_7	50	4.2	0.8	95	234	0.1707	-36.4	48.17
F_8	50	4.1	0.9	95	210.3	0.099	-41.3	46.53
F_9	50	4	1	95	202.6	0.0713	-47.5	43.98

Table 2: IN-VITRO DIFFUSION STUDIES DATA OF FORMULATIONS (F1 to F9): % Cummulative drug release (Mean ± S.D) [n=3].

	F_1	F_2	F_3	F_4	F_5	F_6	F_7	F_8	F_9
0	0 ± 0.00	0 ± 0.00	0 ± 0.00	0 ± 0.00	0 ± 0.00	0 ± 0.00	0 ± 0.00	0 ± 0.00	0 ± 0.00
1	0.72 ± 0.26	0.98 ± 0.43	1.38 ± 1.63	1.60 ±1.12	3.70± 01.98	6.61 ± 0.55	4.07 ± 0.39	4.99 ± 0.40	6.23± 0.12
2	1.86 ± 1.07	2.02 ± 1.36	2.16 ± 0.66	2.35 ±0.16	5.57 ± 1.35	8.41±0.56	5.83 ± 1.73	7.17 ± 1.30	8.37 ± 0.68
3	3.10 ± 1.63	3.55 ± 2.09	3.25 ± 1.56	3.54 ±1.32	7.20 ± 0.28	10.04±0.17	8.04 ± 0.61	9.47 ± 1.36	11.02 ± 0.39
4	4.48 ± 2.42	4.977± 0.13	4.73 ± 1.32	5.02 ±2.16	9.57 ± 1.55	11.86±1.26	10.28 ± 2.06	12.10 ± 1.45	13.68 ± 1.01
5	5.92 ± 1.18	6.88 ± 2.69	6.73 ± 0.44	7.10 ±1.02	11.99± 2.67	14.63±2.51	12.48 ± 0.23	14.76 ± 0.70	16.50 ± 0.99
6	7.80 ± 1.42	8.55 ± 1.23	8.47 ± 0.12	9.44 ±1.58	14.51± 0.30	16.72 ±0.43	15.48 ± 0.19	17.84 ± 1.15	19.78 ± 0.16
7	9.51 ± 2.02	10.93 ± 2.16	10.67± 1.60	11.44 ±0.77	17.28± 0.51	19.48±1.13	18.09 ± 0.70	21.23 ± 0.11	22.91 ± 0.85
8	11.67 ± 2.69	13.75 ± 3.63	12.59±0.97	1345 ±1.13	20.18± 1.71	22.52±1.40	20.81 ± 0.53	24.58 ± 1.39	26.47 ± 1.32
9	14.36 ± 1.25	16.24 ± 2.14	15.0 ± 1.41	15.97 ±1.44	23.12± 2.73	26.57±1.75	24.05 ± 1.34	28.45 ± 0.91	30.31 ± 2.21
10	16.98 ± 3.12	19.33 ± 1.17	17.44± 2.42	18.22 ±2.12	26.52± 2.26	29.76±3.06	27.19 ± 2.41	32.06 ± 0.13	34.32 ± 0.36
11	20.05 ± 0.10	22.73 ± 0.87	19.84± 1.49	20.77 ±0.45	29.65± 1.78	33.26±0.29	30.46 ± 0.66	35.06 ± 0.14	38.24 ± 0.46
12	23.12 ± 3.36	26.11 ± 3.13	22.75± 1.13	23.88 ±0.91	33.27± 3.11	37.18±1.76	34.14 ± 2.45	39.81 ± 0.46	42.96 ± 0.69
24	34.49 ± 0.32	34.14 ± 1.06	31.96± 0.36	32.15 ±3.21	42.22± 0.18	42.75± 0.61	45.13 ± 3.40	50.76 ± 2.31	53.38 ± 2.61
48	44.85 ± 0.17	45.75 ± 2.42	42.91± 0.13	43.75 ±1.56	54.20± 1.15	55.73± 2.30	57.00 ± 2.59	62.04 ± 2.65	65.14 ± 3.44
72	56.10 ± 1.47	59.46 ± 1.02	62.48± 1.33	65.39±1.63	67.58± 0.62	70.95±0.95	72.19 ± 2.07	75.72 ± 1.92	78.26 ± 2.41

Table 3: IN-VITRO DRUG DIFFUSION KINETICS OF FORMULATIONS (F_1- F_9).

	Correlation coefficient (r^2)				Release kinetics			Exponential Coefficient
Formulation Code	Zero Order	First Order	Higuchi	Peppas	K (Hr-1)	T50% (Hr)	K (Hr)	(n)
F1	0.9187	0.9702	0.9448	0.9692	0.0126	55.1	182.9	0.6898
F2	0.9041	0.9677	0.951	0.9658	0.0135	51.2	170.2	0.9999
F3	0.9404	0.9835	0.9466	0.976	0.0136	50.9	169	0.9499
F4	0.9387	0.9827	0.948	0.9754	0.0145	47.9	159.1	0.9258
F5	0.8082	0.9442	0.9751	0.9754	0.0174	32.1	71.8	0.7307
F6	0.7339	0.928	0.9801	0.9755	0.0189	40.5	73	0.9258
F7	0.8223	0.9591	0.9765	0.979	0.0192	30.3	68.2	0.7235
F8	0.7482	0.9413	0.9747	0.9733	0.0218	30.1	97.5	0.6898
F9	0.7076	0.9378	0.9755	0.974	0.0263	27	87.4	0.6489

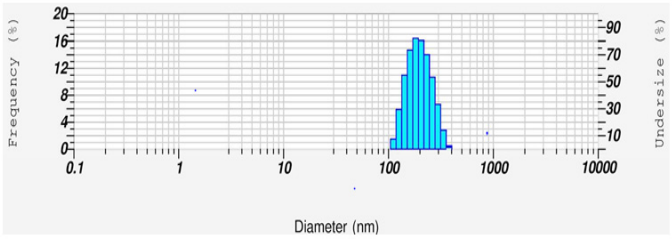

Particle size distribution histogram of F9 584x158mm (96 x 96 DPI)

Figure 1: Particle Size distribution of the formulation F9.

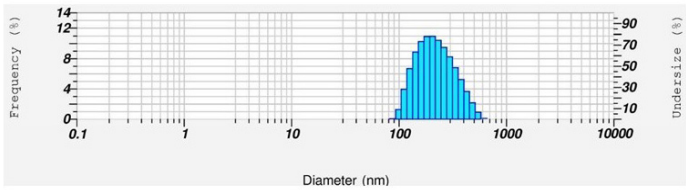

Particle size distribution histogram of F7
584x158mm (96 x 96 DPI)

Figure 2: Particle Size distribution of the formulation F8.

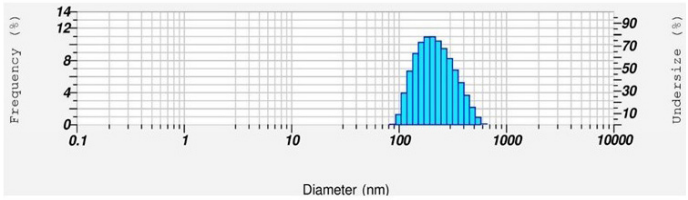

Particle size distribution histogram of F7
584x158mm (96 x 96 DPI)

Figure 3: Particle Size distribution of the formulation F7.

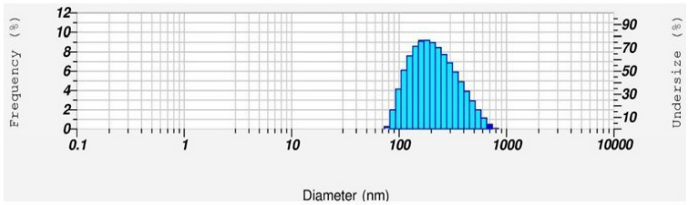

Particle size distribution histogram of F6
584x158mm (96 x 96 DPI)

Figure 4: Particle Size distribution of the formulation F6.

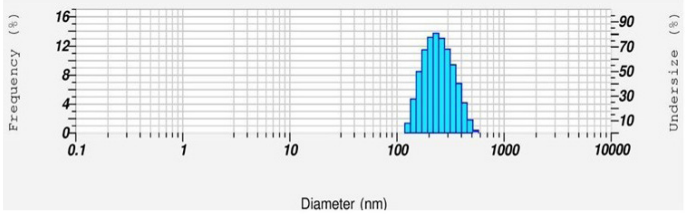

Particle size distribution histogram of F5
584x158mm (96 x 96 DPI)

Figure 5: Particle Size distribution of the formulation F5.

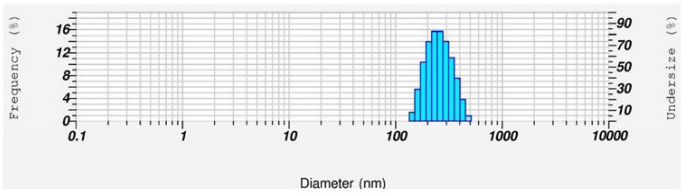

Particle size distribution histogram of F4
584x158mm (96 x 96 DPI)

Figure 6: Particle Size distribution of the formulation F4.

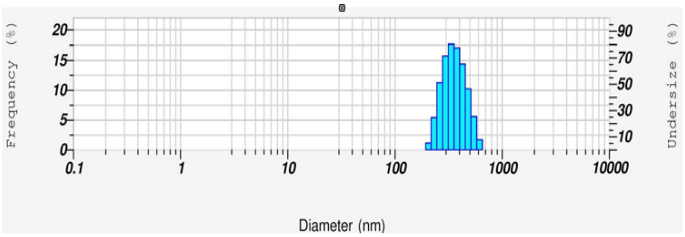

Particle size distribution histogram of F2 584x158mm (96 x 96 DPI)

Figure 7: Particle Size distribution of the formulation F3.

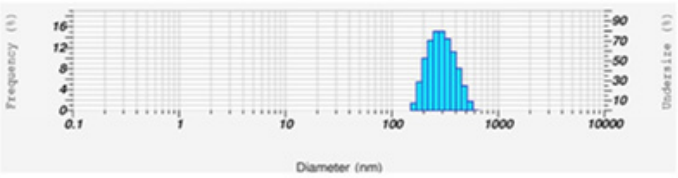

Particle size distribution histogram of F3
584x158mm (96 x 96 DPI)

Figure 8: Particle Size distribution of the formulation F2.

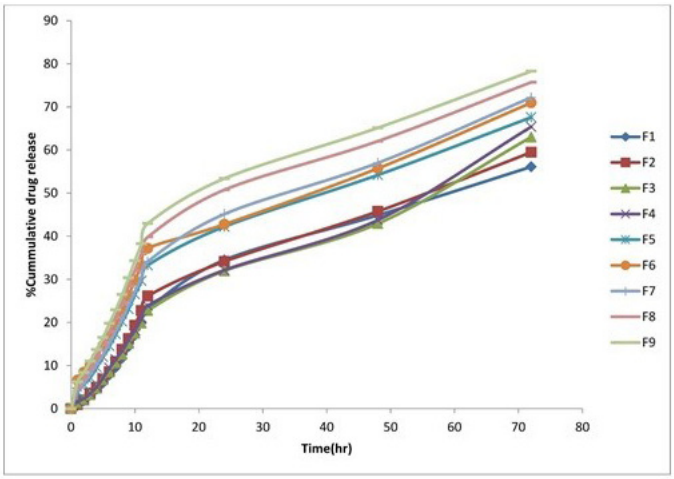

Figure 9: Particle Size distribution of the formulation F1.

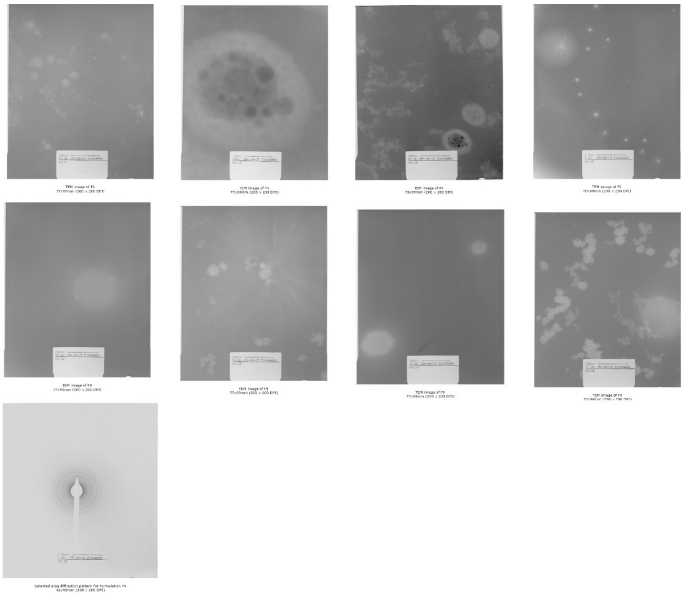

Figure 10: Graph representing the percentage of drug release of various formulations F1 to F9.

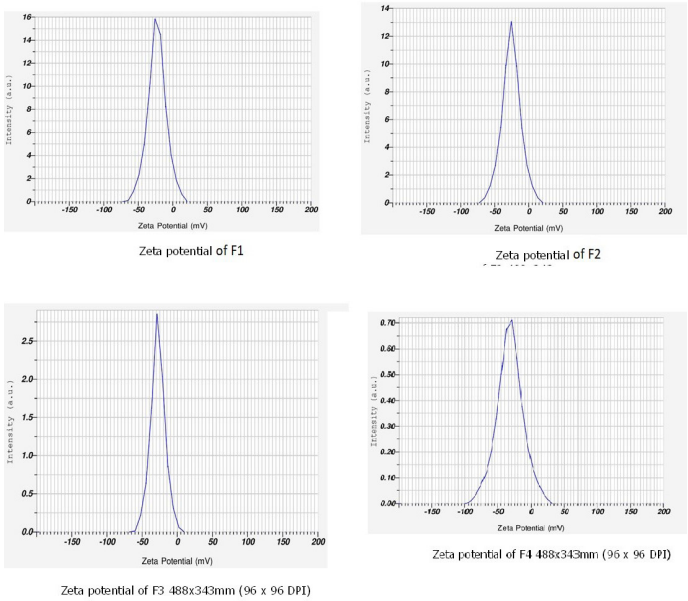

Figure 11: Transmission Electron microscopy of different formulations F1 to F9.

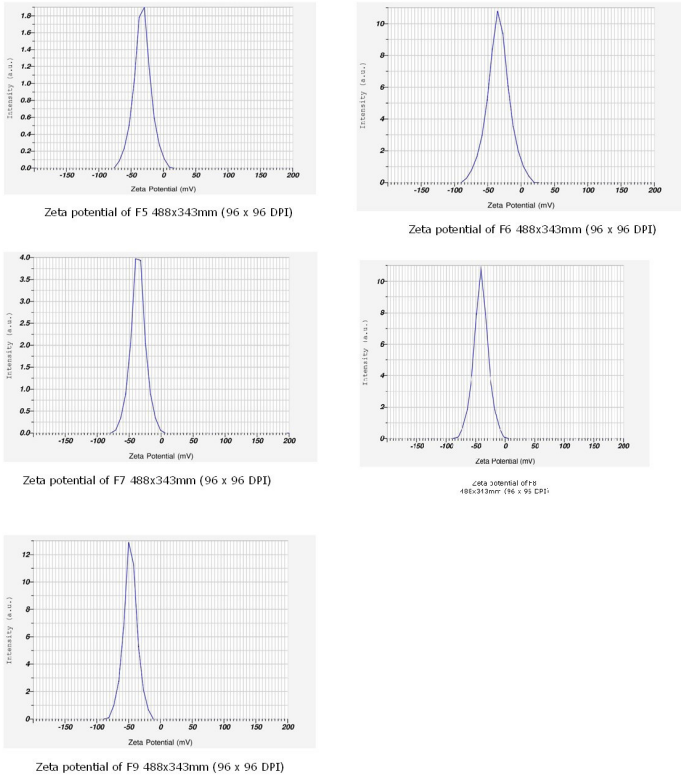

Figure 12: Zeta potential of the different formulations F1 to F9.

Discussion

Liquid crystalline nanoparticle dispersions of lornoxicam using GMO and Lutrol F127 were prepared by employing emulsification followed by high speed homogenization technique. The prepared formulations showed a decrease mean particle size from 367.9nm (F1) to 202.6nm (F9) with a narrow range of polydispersity index. The change in particle size may be attributed to increase in concentration of Lutrol F127 and swelling of phases caused by the excipients used. The zeta potential values of formulations increased gradually from F1 (-23.3mV) to F9 (-47.5mV) indicating moderate to good stability. The length of the hydrophobic chain and type of the head group is vital in determining the structure of liquid crystalline nanoparticles.24 The influence of the concentration of excipients on morphological structure of LCNP'S were determined by performing TEM analysis for F1, F4 and F9 formulations which were selected with respect to high (F1), intermediate (F4) and low (F9) concentrations of GMO used. The TEM micrographs of formulation F1 revealed cubic shaped LCNP'S along with amorphous blobs whereas the micrographs of formulations F4 and F9 showed predominant number of cubic shaped LCNP'S along with fewer reverse hexagonal shaped LCNP'S. The presence of amorphous blobs in F1 may be attributed to the melting of LCNP'S under high energy beam of Transmission electron microscope. Selected Area Electron Diffraction studies were performed for determining the structural organization of LCNP'S, which showed inter planar spacing (d-spacing) of 3.155 Å, 2.422 Å,1.554 Å, 1.4 Å, and 1.293 Å calculated from rings (inner to outer) in the diffraction pattern. From these values it can be deciphered that the particles in formulation (F9) have an FCC (Face Centered Cubic) or HCP (Hexagonal Close Packing) structure. Further validation of structural organization has to be done in order to confirm symmetry. The concentration of GMO had a direct impact on the entrapment efficiencies of the formulations as the entrapment efficiency values decreased from F1 (60.92%) to F9 (43.98%) with respect to decreasing concentrations of Glyceryl monooleate. Whereas the % drug release was vice- versa to entrapment efficiency as it increased from F1 (56.10%) to F9 (78.26%), substantiating that the decrease in concentration of GMO had a impact on entrapment efficiency Both the GMO and Lutrol F127 has a vital role in drug release of Lornoxicam from LCNP'S. The 47% cumulative drug release of lornoxicam from LCNP'S was found to be increased upon increase in the concentration of Lutrol F127 which is attributed to the anchoring of Lutrol F127 at the interface of the lipid bilayer and aqueous phase [9,25]. However the release was slowed down with the increasing proportion of GMO which strongly withholds the drug within the hydrophobic domain of bilayer. Invitro diffusion studies of Lornoxicam LCNP'S revealed that drug release from all the formulations followed first order kinetics ascertaining Peppas mechanism for formulations(F1, F2, F3, F4, F5 &F7) and Higuchi mechanism for formulations (F6, F8 & F9) respectively. Application of Korsmeyer-Peppas equation to the data revealed that mechanism of Lornoxicam liquid crystalline nanoparticles is governed by predominant Non-fickian diffusion (0.5< n <

0.85) for formulations (F1, F5 &F7) and Case-II transport (1 > n > 0.85) for formulations (F2, F3 & F4).The release behavior may be attributed to the type of liquid crystalline phases formed, loading capacity and electrostatic interactions between drugs and lipid bilayer [26].

Conclusion

GMO based Liquid crystalline nanoparticles of Lornoxicam were successfully prepared by employing emulsification followed by homogenization for percutaneous delivery of lornoxicam. The % entrapment efficiency, zeta potential and particle size were directly influenced upon change in concentration of GMO and Lutrol F-127 used. The in-vitro diffusion studies indicated sustained release behavior of lornoxicam from LCNP'S. This approach could provide better penetration of lornoxicam through stratum corneum for the effective management of musculoskeletal and joint disorders like rheumatoid arthritis and osteoarthritis.

References

1. Zhang Y, Zhong D, Si D, Guo Y, Chen X, et al. Lornoxicam pharmacokinetics in relation to cytochrome P450 2C9 genotype, Br J Clin Pharmacol. 2005; 59: 7-14.
2. B. Kidd, W.A. Frenzel. A multicenter, randomized, double blind study comparing lornoxicam with diclofenac in osteoarthritis, J. Rheumatol. 1996; 23: 1605-1611.
3. H. Staunstrup, J. Ovesen, U.T. Larsen, K. Elbaek, U. Larsen, K. Kroner. Efficacy and tolerability of lornoxicam versus tramadol in postoperative pain. J Clin Pharmacol. 1999; 39: 834-841.
4. McCormack KJ. Non-steroidal anti-inflammatory drugs and spinal nociceptive processes.
5. Cashman JN. "The mechanisms of action of NSAIDs in analgesia". Drugs. 1996; 52: 13-23.
6. Zhang Z, Bi X, Li H, Huang G, Enhanced targeting efficiency of PLGA microspheres loaded with Lornoxicam for intra-articular administration.Drug Deliv. 2011; 18: 536-544.
7. Calum J. Drummond, Celesta Fong. Surfactant self-assembly objects as novel drug delivery vehicles. Curr Opin Colloid Interface Sci. 2000; 4: 449-456.
8. Luzzati V, Husson F. The structure of the liquid-crystalline phases of lipid-water systems. J Cell Biol. 1962; 12: 207-219.
9. Spicer PT, Hayden KL, Lynch ML, Ofori-Boateng A, Burns JL. Novel process for producing cubic liquid crystalline nanoparticles (Cubosomes). Langmuir 2001; 1: 5748-5756.
10. Boyd BJ, Whittaker DV, Khoo SM, Davey G. Hexosomes formed from glycerate surfactants-formulation as a colloidal carrier for irinotecan. Int J Pharm. 2006; 318: 154-162.
11. Lynch ML, Ofori-Boateng A, Hippe A, Kochvar K, Spicer PT. Enhanced loading of water-soluble actives into bicontinuous cubic phase liquid crystals using cationic surfactants. J Colloid Interface Sci. 2003; 260: 404-413.
12. Cosmetic Ingredient Review Panel. Final report on the safety assessment of glyceryloleate. J Am Coll Toxic. 1986; 5: 391-413.
13. Appel L, Engle K, Jensen J, Rejewski L, Zentner G. An in vitro model to mimic in vivo subcutaneous monoolein degradation. Pharm Res. 1994; 11: S217.
14. Ogiso T, Masahiro I, Paku T. Effect of various enhancers of transdermal penetration of indomethacin and urea and relationship between penetration parameters and enhancement factors. J Pharm Sci. 1995; 84: 482-488.
15. Moser K, Kriwet K, Naik A, Kalia YN, Guy RH. Passive skin penetration enhancement and its quantification in vitro. Eur J Pharm Bipharm. 2001; 82: 103-112.
16. N. Lars, Ashraf AA. Stratum corneum keratin structure,function, and formation: the cubic rod-packing and membrane templating model. J Invest Dermatol. 2004; 4: 715-732.
17. Jain R, Jain V, Kohli DV. Hexosomes: a tool for transdermal delivery of poorly water soluble drug. XVIII International Conference on Bioencapsulation – Porto. Portugal, 2010.
18. Elisabetta Esposito, Rita Cortesi, Markus Drechsler, Lydia Paccamiccio, Paolo Mariani, Catia Contado, et al. Cubosome Dispersions as Delivery Systems for Percutaneous Administrationof Indomethacin Pharmaceutical Research. 2005; 22.
19. Jaina V, Swarnakara NK, Mishrab PR, Vermab A, Kaulc A, et al. Paclitaxel loaded PEGylated gleceryl monooleate based nanoparticulate carriers in chemotherapy. Biomaterials. 2012; 33: 7206-7220.
20. Wasana Chaisria, Wim E. Henninkb, Siriporn Okonogia. Preparation and Characterization of Cephalexin Loaded PLGA Microspheres. Current Drug Delivery. 2009; 6: 69-75.
21. Hackley VaF CF. The use of nomenclature in dispersion science and technology, NIST recommended practice guide. SP. 2001; 960: 76.
22. Di Bei, Tao Zhang, James B. Murowchick, Bi-Botti C. Youan. Formulation of Dacarbazine-loaded Cubosomes. Part III. Physicochemical Characterization AAPS PharmSciTech. 2010; 11: 1243-1249.
23. Deepak Kumbhar, Preeti Wavikar, Pradeep Vavia. Niosomal Gel of Lornoxicam for Topical Delivery: In vitro Assessment and Pharmacodynamic Activity. AAPS PharmSciTech. 2013; 14:1072-1083.
24. Chang CM, Bodmeier R. Binding of drugs to monoglyceride-based drug delivery systems. Int J Pharm. 1997; 147: 135-142.
25. Gustafsson J, Ljusberg-Wahren H, Almgren M, Larsson K. Submicron particles reversed lipid phases in water stabilized by a nonionic amphiphilic polymer. Langmui. 1997; 13: 6964-6971.
26. Chenyu Guo, Jun Wang, Fengliang Cao, Robert J. Lee, Guangxi Zhai. Lyotropic liquid crystal systems in drug delivery. Drug Discovery Today. 2010; 15: 1032-1040.